Sr$_4$PbPt$_4$O$_{11}$, the first platinum oxide containing Pt$_2^{6+}$ ions

Catherine Renard*, Pascal Roussel, Annick Rubbens,
Sylvie Daviero-Minaud, Francis Abraham

*Unité de Catalyse et de Chimie du Solide, équipe de Chimie du Solide (CNRS UMR 8181) ENSC Lille–UST Lille, BP 90108,
59652 Villeneuve d'Ascq cedex, France*

Abstract

We report the synthesis and crystal structure of the new compound Sr$_4$PbPt$_4$O$_{11}$, containing platinum in highly unusual square pyramidal coordination. The crystals were obtained in molten lead oxide. The structure was solved by X-ray single crystal diffraction techniques on a twinned sample, the final R factors are $R = 0.0260$ and w$R = 0.0262$. The symmetry is triclinic, space group $P\bar{1}$, with $a = 5.6705(6)$ Å, $b = 9.9852(5)$ Å, $c = 10.0889(5)$ Å, $\alpha = 90.421(3)°$, $\beta = 89.773(8)°$, $\gamma = 90.140(9)°$ and $Z = 2$. The structure is built from dumbbell-shaped Pt$_2$O$_9$ entities formed by a dinuclear metal–metal bonded Pt$_2^{6+}$ ion with asymmetric environments of the two Pt atoms, classical PtO$_4$ square plane and unusual PtO$_5$ square pyramid. Successive Pt$_2$O$_9$ entities deduced from 90° rotations are connected through the oxygens of the PtO$_4$ basal squares to form [Pt$_4$O$_{10}^{8-}$]$_\infty$ columns further connected through Pb^{2+} and Sr^{2+} ions. Raman spectroscopy confirmed the peculiar platinum coordination environment.
© 2006 Elsevier Inc. All rights reserved.

Keywords: Platinum oxide; Pt$_2^{6+}$ ion; 5-coordinated platinum; Crystal structure; X-ray diffraction

1. Introduction

Many binary and ternary platinum oxides have already been chemically and structurally studied for several reasons: (1) numerous alkaline, alkaline earth, post transition metals (Pb, Bi,…) platinum oxides were formed when platinum, a chemically inert and stable to high temperature metal, was used as a container for synthesis experiments using the corresponding melted oxides, (2) they exhibit a large range of electronic properties (3) platinum presents several oxidation states, (4) some oxides are of technical interest due to their catalytic and electrochemical properties and their potential applications as, for example, H$_2$–O$_2$ fuel-cell electrocatalysts. From a structural point of view, platinum oxides can be divided into two groups: those containing divalent (Pt^{2+}) or partially oxidized platinum in planar coordination and those with fully oxidized tetravalent platinum (Pt^{4+}) in octahedral coordination [1]. In many partially oxidized platinum oxides, the PtO$_4$ squares are

stacked and the compounds exhibit strong metal–metal interactions leading to electronic delocalization along the Pt–Pt chains and highly conducting materials. Similar behaviour is observed in partially oxidized one-dimensional tetracyano-platinates.

Previous studies on compounds of the Pb/Pt/O system allowed us to synthesize two lead platinum oxides, Pb$_2$PtO$_4$ [2] and PbPt$_2$O$_4$ [3]. The first one contains Pt^{4+} in octahedral coordination, the PtO$_6$ octahedra are edge-shared to form rutile-type chains further connected through Pb^{2+} ions. The structure of the latter consists of PtO$_6$ octahedra (Pt^{4+}) and two types of PtO$_4$ square planes containing divalent and/or partially oxidized platinum. Partial substitution of Bi^{3+} for Pb^{2+} is achieved in Pb$_{1-x}$Bi$_x$Pt$_2$O$_4$ ($0 \leqslant x \leqslant 0.3$) by partial reduction of platinum in the [PtO$_4$] chains [4]. Although Bi$_2$PtO$_4$ has not been isolated, a series Bi$_{2-x}$Pb$_x$PtO$_4$ has been stabilized within the range $0.33 \leqslant x \leqslant 0.52$ [5–7] by partial oxidation of Pt^{2+} in [PtO$_4$] infinite chains to give a structure similar to that of Bi$_2$CuO$_4$ [8] and Bi$_2$PdO$_4$ [9].

In the Sr/Pt/O system, only Sr$_4$PtO$_6$ with K$_4$CdCl$_6$ type structure and isolated PtO$_6$ octahedra has been reported

---

*Corresponding author. Fax: +33 3 20 43 68 14.
E-mail address: catherine.renard@ensc-lille.fr (C. Renard).

[10–12]. Substitution of one Sr by divalent metals, Mg [13,14], Ni [15,16], Cu [16–18], Zn [19], leads to the largely studied Sr_3MPtO_6 series. Attempts to substitute Sr by Pb were unsuccessful due to the unfavorable environment of M atom for the lone pair Pb^{2+} ion. However in the course of the investigation of the Sr/Pb/Pt/O system we have isolated $Sr_4PbPt_4O_{11}$, a new compound containing dinuclear metal–metal bonded platinum (III) dumbbell-shaped Pt_2^{6+} ions, evidenced for the first time in an oxide compound. This paper reports the synthesis, the crystal structure determination and Raman spectroscopy study of this unique platinum (III) oxide.

2. Experimental

2.1. Synthesis

Crystals of $Sr_4PbPt_4O_{11}$ were prepared in molten PbO as a flux. Strontium carbonate, platinum and lead oxide in proportion 2:1:5 were ground and placed in a gold crucible. The mixture was heated at $930\,°C$ for 3 h, and then slowly cooled down to $850\,°C$ at $1\,°C\,h^{-1}$ whereupon the furnace is turned off and allowed to cool down to room temperature. The crystals were extracted from the flux by dissolving PbO in excess in hot acetic acid, isolated by filtration and rinsed with distilled water. All the crystals are black, thin needles. The reference compounds chosen for Raman spectroscopy were synthesized as described in the referenced publications; Sr_4PtO_6 [10], and $PbPt_2O_4$ [3] were prepared via solid state reaction and $Bi_{1.6}Pb_{0.4}PtO_4$ [5] crystals were obtained in molten $PbO–Bi_2O_3$.

2.2. EDS elemental analysis

A quantitative elemental analysis was performed by Energy Dispersive Spectroscopy (EDS), with a Jeol JSM–5300 scanning microscope equipped with a IMIX system of Princeton Gamma technology, at 15 kV. Strontium, lead and platinum percentages were calibrated with standards.

2.3. Thermal analysis

The thermal stability of $Sr_4PbPt_4O_{11}$ was studied by thermal differential analysis performed with a TG/DT 92 SETARAM instrument from room temperature to $1100\,°C$ under air, the decomposition compounds were identified by X-ray powder diffraction.

2.4. X-ray diffraction

A black needle crystal of $Sr_4PbPt_4O_{11}$ was mounted on a glass fibre and aligned on a Bruker X8 Apex II CCD 4 K diffractometer. The X-rays intensity data were collected at room temperature using a $MoK\alpha$ radiation ($\lambda = 0.71073\,Å$) selected by a graphite monochromator. The raw data frames were integrated with SAINT program [20], which

also applies corrections for Lorentz and polarization effects. Due to the fineness of the needle, a semi-empirical absorption correction was applied using the program SADABS [21], based on redundancy. The positions of the heavy atoms (Sr, Pb and Pt) were determined by direct method using SIR97 [22], and then refined on $|F|$ using JANA2000 [23], the oxygen atoms were localized on the Fourier difference maps. The crystallographic and experimental details are summarized in Table 1.

The powder X-ray diffraction pattern was collected on ground crystals, using a Bruker D8 diffractometer, with $CuK\alpha$ radiation ($\lambda = 1.54056\,Å$) and an energy dispersive detector (sol-X). The profile fitting and the cell parameters refinements were performed using the powder option of JANA2000 [23].

Table 1
Crystallographic data and experimental details for $Sr_4PbPt_4O_{11}$ structure determination

Crystal data	
Formula	$Sr_4PbPt_4O_{11}$
Formula molar weight	1513.98
Z	2
Unit cell dimensions	
a (Å)	5.6705 (6)
b (Å)	9.9852 (5)
c (Å)	10.0889 (5)
α (°)	90.421 (3)
β (°)	89.773 (8)
γ (°)	90.140 (9)
V (Å^3)	571.22 (8)
Calculated density (g cm^{-3})	8.799 (1)
Data collection	
Theta range (°)	2.02–42.35
Index range	$-7 \leqslant h \leqslant 9$; $-18 \leqslant k \leqslant 18$; $-19 \leqslant l \leqslant 18$
Reflections collected	25363
Reflections observed	22713
Independent reflections	6584
Independent reflections $>3\sigma(I)$	5852
Redundancy	3.852
Criterion for observation	$I>3\sigma(I)$
Refinement	
Data/restraints/parameters	6584/0/128
Final R indices (R, wR) all	3.10, 2.67
Final R indices (R wR) obs	2.60, 2.62
Weighting scheme	$1/\sigma^2(F)$
Twinning matrix	$\begin{pmatrix} 1 & 0 & 0 \\ 0 & \bar{1} & 0 \\ 0 & 0 & \bar{1} \end{pmatrix}$
Twin ratio	26.74%
Largest diff. peak and hole [e Å^3]	2.67 (0.62 Å from Pt(1)), -2.31 (0.35 Å from Pb(1))
Extinction method	Becker and Coppens [24]
Extinction coefficient	0.00058(2)

$R = \sum(|F_0| - |F_C|)/\sum|F_0|$, w$R = [\sum w(|F_0^2| - |F_C^2|)^2/\sum w(F_0^2)^2]^{1/2}$, $w = 1/[\sigma^2(F_0^2) + (aP)^2 + bP]$ where a and b are refinable parameters and $P = (F_0^2 + 2F_C^2)/3$.

2.5. Raman spectroscopy

The Raman spectra were obtained at room temperature with the 647.1 nm excitation line from a Spectra Physics krypton ion laser. The beam was focused onto the sample using the microscopic configuration of the apparatus. The scattered light was analysed with an XY Raman Dilor spectrometer equipped with an optical multichannel charge coupled device liquid nitrogen-cooled detector. In the $140–1000\,cm^{-1}$ required range, the spectral resolution is approximately $0.5\,cm^{-1}$. The Raman spectra of four platinum oxides were measured: $Sr_4PbPt_4O_{11}$, Sr_4PtO_6, $Bi_{1.6}Pb_{0.4}PtO_4$ and $PbPt_2O_4$. The last three compounds were chosen as references for their specific platinum environment coordination. Sr_4PtO_6 [10–12] contains only octahedral coordinated platinum atoms, the transition metal adopts only square plane environment in $Bi_{1.6}Pb_{0.4}PtO_4$ [5–7] and the $PbPt_2O_4$ [3] crystal structure combines both octahedral and square planar platinum coordinations.

3. Results and discussion

3.1. Structure refinement

The unit cell parameters indicated a pseudo-tetragonal system, the tetragonal and orthorhombic symmetry were quickly ruled out by a simple examination of the averaging agreement factor. The different settings in the monoclinic symmetry were tested: $R_{int} = 0.4294$, 0.4415 and 0.0894 for $112/m$, $12/m1$, and $2/m11$, respectively, with cell parameters given in Table 1. Then, at this level, the structure was solved in the monoclinic system with cell parameters $a = 9.9852(5)\,Å$, $b = 5.6705(6)\,Å$, $c = 10.0889(5)\,Å$ and $\beta = 90.421(3)°$. As the set of reflections did not evidence any systematic extinction, space groups $P2/m$, Pm and $P2$ were tested. The atomic positions are almost related by a 2_1 axis, thus despite the absence of systematic extinction, the structure refinement was undertaken in $P2_1$ and $P2_1/m$ space groups, trying different twin possibilities. The best results were obtained in Pm with final $R = 0.0742$ and $wR = 0.0899$, but with negative isotropic displacement parameters for some oxygen atoms and disorder for others. The low quality of these results questioned the choice of the crystal system. The cell parameters were then refined from powder X-ray diffraction considering monoclinic and triclinic systems. Refinement in the triclinic system, with $R_p = 0.0877$ and $\chi^2 = 1.93$, was better compared to that in the monoclinic cell, $R_p = 0.1008$, $\chi^2 = 2.45$. The observed and calculated diffraction patterns are shown in Fig. 1, the most relevant difference between the monoclinic and triclinic refinement is pointed out in the insert. The refined cell parameters are $a = 5.6705(6)\,Å$, $b = 9.9852(5)\,Å$, $c = 10.0889(5)\,Å$, $\alpha = 90.421(3)°$, $\beta = 89.773(8)°$ and $\gamma = 90.140(9)°$. The structure determination was then undertaken in $P\bar{1}$ space group. The direct methods lead to the similar crystal structure than in Pm space group and the refinement gave $R = 0.0895$ and $wR = 0.1283$. At this point, it is clear that the structure is pseudo-symmetric. Different merohedric twin possibilities (i.e. completely overlapped ones) were then tested and the volume fraction of the second element was refined. The structure factor for complete overlapping is calculated as $F^2(H) = vF^2(HT_1) + (1 - v)F^2(H)$ where v is the volume fraction and T the matrix representation of the twin operator. In our case, $T = [100,0\bar{1}0,00\bar{1}]$ corresponds to a pseudo-mirror perpendicular to $a*$, i.e. the symmetry element lost during the passage from monoclinic $2/m11$ to triclinic $\bar{1}$ symmetries. Subsequently, the refinement was meaningfully improved, $R = 0.026$ and $wR = 0.0262$ and twin ratio $v = 0.267$. Note that this twin was systematically observed on the different crystals tested. The anisotropic displacement parameters were allowed to vary for Sr, Pb and Pt atoms, the displacement parameters for the oxygen atoms were kept isotropic. The formulae deduced from the crystal structure refinement is in good accordance with the EDS analysis performed on single crystal which indicated Sr:Pb:Pt ratio close to 4:1:4 and no other element.

The final atomic coordinates and displacement parameters are given in Tables 2 and 3, respectively. Table 4 reports the main interatomic distances and angles.

3.2. Platinum polyhedra

There are four crystallographically independent Pt atoms in $Sr_4PbPt_4O_{11}$, each is coordinated by four oxygen atoms forming a square with Pt–O distances ranging from 2.005(5) to 2.046(5) Å. For Pt(2) and Pt(3), the coordination polyhedra is completed by a fifth oxygen atom at a shorter distance, 1.993(4) and 1.984(4) Å for Pt(2) and Pt(3), respectively, forming a square pyramid. The average Pt–O distances are slightly larger for four-coordinated platinum Pt(1) and Pt(4), 2028(8) and 2.025(12) Å, respectively, than for five-coordinated Pt(2) and Pt(3), 2.015(13) and 2.016(25) Å, respectively. Planar coordination for platinum is common to many oxides. Five-coordinated platinum atoms have been reported in platinum complexes in trigonal bipyramid [25,26] or square pyramid [27] environments but $Sr_4PbPt_4O_{11}$ is the first platinum oxide, to our knowledge, containing five-coordinate platinum.

3.3. Structural connectivity

The projection of the structure of $Sr_4PbPt_4O_{11}$ along [100] is presented in Fig. 2. The structure can be described as built from $[Pt_4O_{10}^{8-}]_\infty$ columns running down [100] and separated by Sr^{2+} and Pb^{2+} ions. The columns consist of corner shared square planes PtO_4 and square pyramids PtO_5. Each square plane is opposite to a square pyramid; this set constitutes the elemental building unit (EBU) Pt_2O_9 and is reproduced with a rotation angle of about 90°. The successive EBU are linked by sharing the corners of the squares (Fig. 3). Two different EBU are formed, $Pt(1)Pt(2)O_9$ and $Pt(3)Pt(4)O_9$. Whatever the platinum
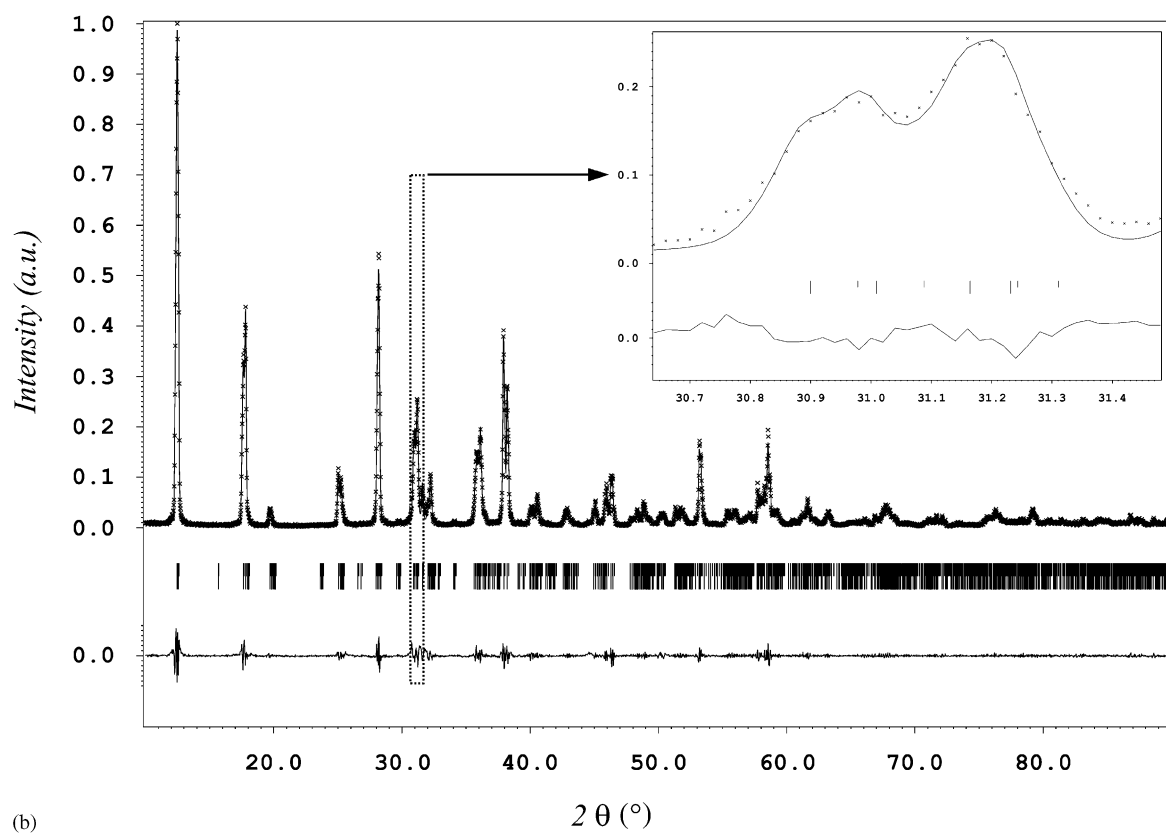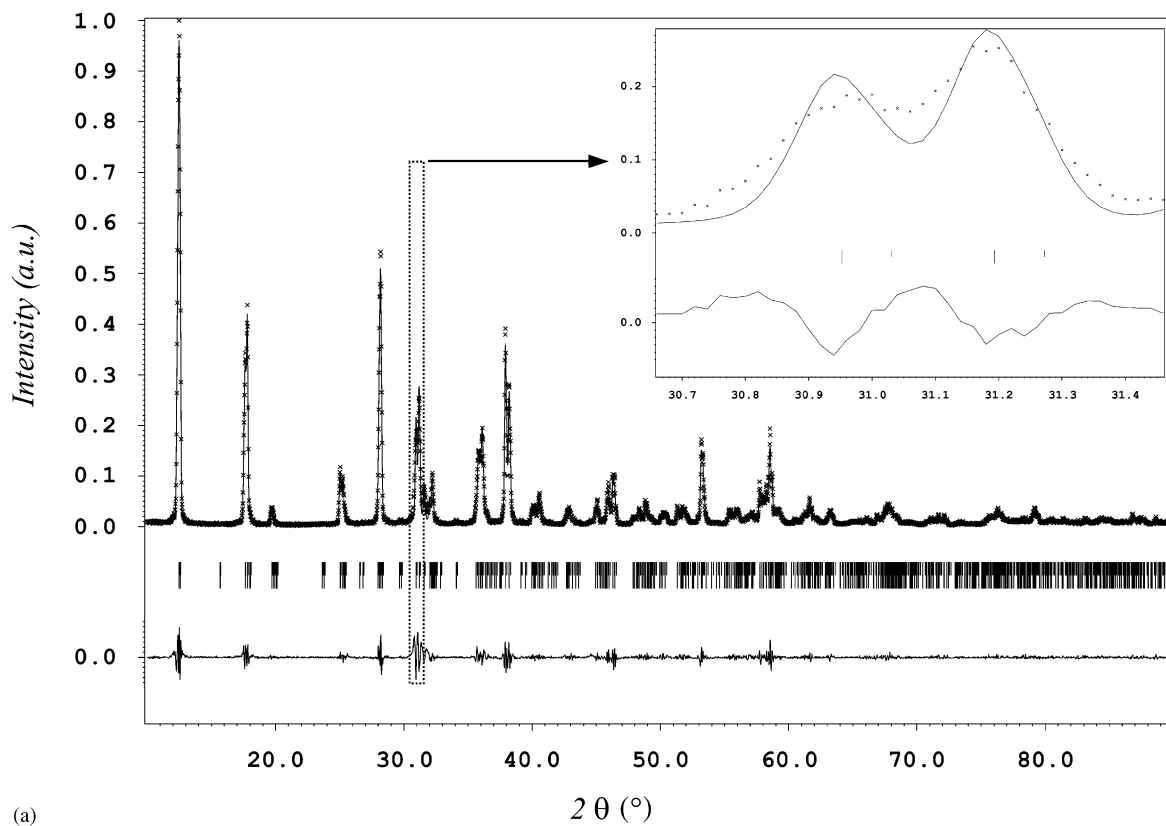
Fig. 1. Observed and calculated diffraction patterns of $Sr_4PbPt_4O_{11}$ in monoclinic (a) and triclinic (b) systems. The inset points out the 30.65–31.46° 2θ range.

Table 2
Final atomic coordinates and equivalent isotropic displacement parameters for $Sr_4PbPt_4O_{11}$

	Wick.	Occ	x	y	z	U_{eq}
Pt(1)	2i	1	0.25019(5)	0.202433(18)	−0.107143(18)	0.00683(11)
Pt(2)	2i	1	0.25093(5)	0.293266(18)	−0.355274(18)	0.00648(11)
Pt(3)	2i	1	−0.24965(5)	0.122251(17)	−0.277462(18)	0.00652(11)
Pt(4)	2i	1	−0.24934(5)	0.372350(18)	−0.184564(18)	0.00691(11)
Pb(1)	2i	1	−0.28261(4)	−0.25565(2)	−0.27002(2)	0.01206(10)
Sr(1)	2i	1	0.24977(12)	0.53435(4)	−0.12683(5)	0.0088(3)
Sr(2)	2i	1	0.24879(13)	−0.03523(5)	−0.39433(5)	0.0141(3)
Sr(3)	2i	1	−0.24903(12)	0.12503(5)	0.04821(5)	0.0103(3)
Sr(4)	2i	1	0.24862(12)	−0.38574(5)	−0.48205(5)	0.0127(3)
O(1)	2i	1	−0.4887(8)	0.1686(4)	−0.4156(5)	0.0065(8)
O(2)	2i	1	0.4989(8)	0.4320(4)	−0.3107(5)	0.0068(8)
O(3)	2i	1	0.0051(8)	0.4331(4)	−0.3111(4)	0.0065(8)
O(4)	2i	1	0.4950(8)	0.0604(4)	−0.1490(5)	0.0070(8)
O(5)	2i	1	−0.2459(8)	−0.0566(4)	−0.3643(4)	0.0100(7)
O(6)	2i	1	0.5018(8)	0.3321(5)	−0.0453(5)	0.0071(8)
O(7)	2i	1	−0.0032(8)	0.3329(5)	−0.0436(5)	0.0073(8)
O(8)	2i	1	0.0082(8)	0.0598(4)	−0.1512(5)	0.0078(8)
O(9)	2i	1	−0.0123(8)	0.1720(4)	−0.4164(5)	0.0063(8)
O(10)	2i	1	0.3296(7)	−0.2524(4)	−0.2630(4)	0.0079(7)
O(11)	2i	1	0.2498(8)	0.3664(4)	−0.5384(4)	0.0076(7)

$U_{eq} = \frac{1}{3} \sum_i \sum_j U_{ij} a_i^* a_j^* a_i a_j$.

Table 3
Anisotropic displacement parameters of metal atoms for $Sr_4PbPt_4O_{11}$

	U_{11}	U_{22}	U_{33}	U_{12}	U_{13}	U_{23}
Pt(1)	0.00520(10)	0.00394(7)	0.00308(7)	0.00130(9)	−0.00009(9)	0.00096(5)
Pt(2)	0.00500(10)	0.00321(7)	0.00291(7)	0.00131(9)	−0.00018(9)	0.00085(5)
Pt(3)	0.00506(10)	0.00317(7)	0.00282(7)	0.00117(9)	−0.00006(9)	0.00012(5)
Pt(4)	0.00514(10)	0.00343(7)	0.00370(8)	0.00128(9)	−0.00005(9)	−0.00007(5)
Pb(1)	0.00898(10)	0.00779(8)	0.00581(8)	0.00062(9)	−0.00006(9)	0.00102(6)
Sr(1)	0.0070(2)	0.00390(17)	0.00344(18)	0.0008(2)	0.0000(2)	−0.00035(13)
Sr(2)	0.0111(3)	0.00496(18)	0.0064(2)	0.0020(2)	−0.0008(2)	0.00120(15)
Sr(3)	0.0081(3)	0.00445(17)	0.00434(19)	0.0016(2)	0.0000(2)	0.00116(14)
Sr(4)	0.0100(3)	0.00502(18)	0.00552(19)	0.0012(2)	−0.0007(2)	−0.00010(14)

coordination environment, the metal is slightly moved toward the centre of the column, bending O–Pt–O angles to 172.7–174.7° and creating short Pt–Pt distance of 2.6712(3) and 2.6613(3) Å for Pt(1)–Pt(2) and Pt(3)–Pt(4), respectively. Such distances involve strong metal–metal interactions, with a bonding between the platinum atoms, thus the EBU can be considered as formed by dinuclear Pt_2^{6+} ions with asymmetric environments of the two platinum atoms. $Sr_4PbPt_4O_{11}$ is the first example of platinum oxide containing such a 'lantern dimer' Pt_2O_9. One can note that dinuclear Re_2^{8+} ions within square planes dimers have been reported, in particular in $La_6Re_4O_{18}$ [28] and $La_4Re_2O_{10}$ [29]. In those compounds, the rhenium atoms are also apart from the oxygen square plane, creating a short metal–metal distance.

Several platinum sulphates [30,31], hydrogenophosphates [32–34] and phosphites [35] contain Pt_2^{6+} dumbbell units formed by two square pyramidal coordinated Pt^{3+} ions. The intermetallic distance, in the range from 2.46 to 2.53 Å, depending on the compounds, is imposed by the SO_4^{2-} or hydrogenophosphates bridges. These distances are very short compared to those observed in $Sr_4PbPt_4O_{11}$, however in this oxide the two Pt are not bridged and the Pt–Pt distances are comparable to the values obtained in diplatinum (III) complexes with unsupported Pt–Pt bonds, typically 2.6964(5) and 2.694(1) Å in tetrakis (-dioximato) [36] and imino-hydroxy-dimethylpropane (-trichloro) [37] platinum (III) complexes.

In several oxides, Pt–Pt bonding appears in columnar stacked fourfold planes with one-dimensional interactions like in $Na_xPt_3O_4$ [38–40], $Bi_{1.6}Pb_{0.4}PtO_4$ [5], $PbPt_2O_4$ [3] with metal–metal distances homogeneous along the chains. In PtO [41] or $CaPt_2O_4$ [42], PtO_4 planes are stacked in two perpendicular directions with an unique Pt–Pt distance of

Table 4
Main interatomic distances and angles in $Sr_4PbPt_4O_{11}$

| Bond	Dist. (Å)	Bond	Dist. (Å)	Bond	Dist. (Å)
Pt(1)–O(4)	2.028(4)	Pb(1)–O(5)	2.219(4)	Sr(3)–O(4)	2.547(5)
Pt(1)–O(6)	2.022(5)	Pb(1)–O(10)	2.200(4)	Sr(3)–O(4)	2.532(4)
Pt(1)–O(7)	2.040(5)	Pb(1)–O(11)	2.229(4)	Sr(3)–O(6)	2.687(5)
Pt(1)–O(8)	2.023(4)	Sr(1)–O(2)	2.539(5)	Sr(3)–O(7)	2.667(5)
Pt(2)–O(1)	2.023(4)	Sr(1)–O(3)	2.529(4)	Sr(3)–O(8)	2.563(5)
Pt(2)–O(2)	2.021(4)	Sr(1)–O(6)	2.617(5)	Sr3)O–(8)	2.531(4)
Pt(2)–O(3)	2.022(4)	Sr(1)–O(6)	2.600(5)	Sr(3)–O(10)	2.547(4)
Pt(2)–O(9)	2.016(4)	Sr(1)–O(7)	2.610(5)	Sr(4)–O(1)	2.762(4)
Pt(2)–O(11)	1.993(4)	Sr(1)–O(7)	2.575(5)	Sr(4)–O(2)	2.898(5)
Pt(3)–O(1)	2.007(5)	Sr(1)–O(10)	2.581(4)	Sr(4)–O(2)	2.571(5)
Pt(3)O(4)	2.038(5)	Sr(2)–O(1)	2.528(4)	Sr(4)–O(3)	2.859(4)
Pt(3)–O(5)	1.984(4)	Sr(2)–O(1)	2.694(5)	Sr(4)–O(3)	2.581(4)
Pt(3)–O(8)	2.046(5)	Sr(2)–O(4)	2.998(5)	Sr(4)–O(9)	2.731(4)
Pt(3)–O(9)	2.005(5)	Sr(2)–O(5)	2.828(5)	Sr(4)–O(10)	2.615(4)
Pt(4)–O(2)	2.011(5)	Sr(2)–O(5)	2.891(5)	Sr(4)–O(11)	2.536(4)
Pt(4)–O(3)	2.019(4)	Sr(2)–O(5)	2.611(4)	Sr(4)–O(11)	2.840(5)
Pt(4)–O(6)	2.030(5)	Sr(2)–O(8)	2.956(5)	Sr(4)–O(11)	2.859(5)
Pt(4)–O(7)	2.039(5)	Sr(2)–O(9)	2.559(4)		
Pt(1)–Pt(2)	2.6712(3)	Sr(2)–O(9)	2.700(5)		
Pt(3)–Pt(4)	2.6613(3)	Sr(2)–O(10)	2.593(4)		
Angles	(°)	Angles	(°)	Angles	(°)
O(4)–Pt(1)–O(7)	172.9(2)	O(1)–Pt(3)–O(8)	173.69(18)	O(5)–Pb(1)–O(10)	95.19(16)
O(6)–Pt(1)–O(8)	173.5(2)	O(4)–Pt(3)–O(9)	174.70(18)	O(5)–Pb(1)–O(11)	93.47(15)
O(1)–Pt(2)–O(3)	173.26(17)	O(2)–Pt(4)–O(7)	172.90(19)	O(10)–Pb(1)–O(11)	96.68(16)
O(2)–Pt(2)–O(9)	172.68(18)	O(3)–Pt(4)–O(6)	173.13(18)		
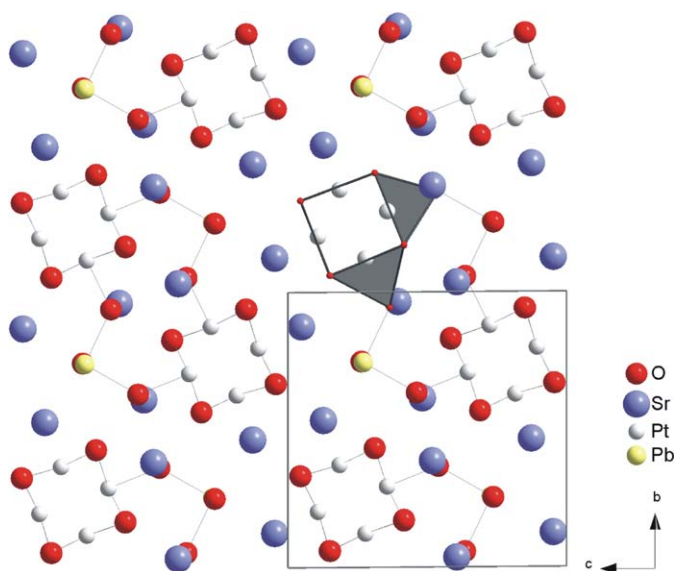
Fig. 2. Projection of the structure of $Sr_4PbPt_4O_{11}$ along [100]. A $[Pt_4O_8^{8-}]_\infty$ column is pointed out with the platinum environment polyhedra.

Fig. 3. The two different asymmetric dumbell-shaped Pt_2O_9 elemental building units (a and b) and their connection to form $[Pt_4O_{10}^{8-}]_\infty$ columns connected by lead atoms (c).

3.04 Å in PtO and with alternating Pt–Pt distances of 2.79(5) and 2.99(5) Å in $CaPt_2O_4$. This last compound has several structural similarities with $Sr_4PbPt_4O_{11}$. The most evident resemblance is the $[Pt_4O_8^{4-}]_\infty$ column consisting on corner-shared platinum square planes (Fig. 4). The platinum atoms are also moved toward the centre of the column, with a O–Pt–O angle of 171° and creating the
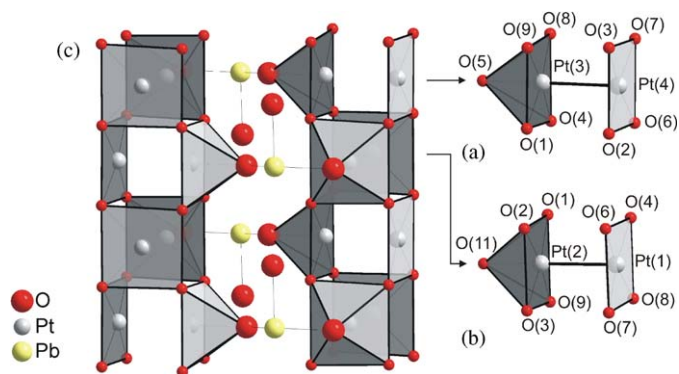
shorter Pt–Pt distance. The second Pt–Pt interaction (2.99 Å) appears between the columns. The Ca^{2+} ions surround the columns with helicoidally 4_2 related positions. A quasi-4_2 symmetry links as well Sr^{2+} coordinates around $[Pt_4O_{10}^{8-}]_\infty$ columns in the triclinic $Sr_4PbPt_4O_{11}$ structure. However the coordination environments of the two alkaline-earth ions are different since the relative columns positions are different in the two structures. The Sr(1) and Sr(3) atoms are seven-coordinated (Fig. 5b) and Sr(2) and Sr(4) are ten-coordinated (Fig. 5a) with oxygen atoms. The seven coordination environment of Sr(1) and Sr(3) can be deduced from the ten coordination environment of Sr(2) and Sr(4) by removing the three oxygen atoms coming
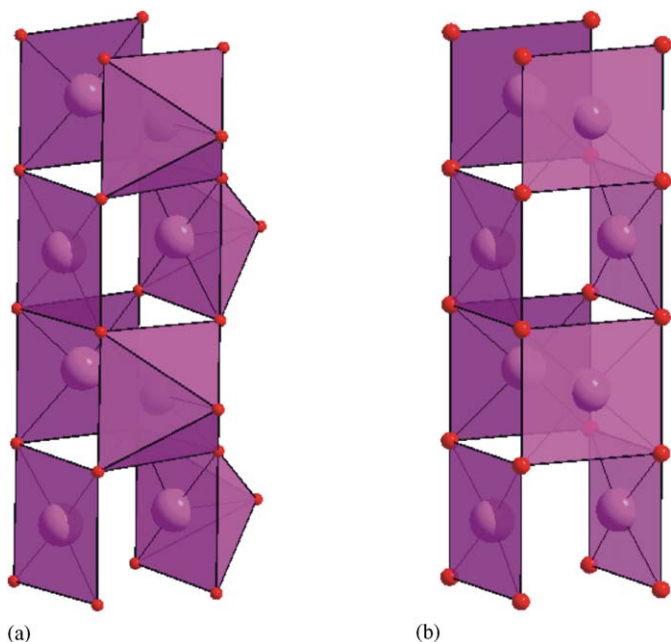
Table 5
Bond valence calculation for cations in $Sr_4PbPt_4O_{11}$

Atom	Supposed bond valence	Calculated bond valence
Pt(1)	+2	1.98
Pt(1)	+4	2.67
Pt(2)	+2	2.57
Pt(2)	+4	3.46
Pt(3)	+2	2.57
Pt(3)	+4	3.46
Pt(4)	+2	2.00
Pt(4)	+4	2.70
Pb(1)	+2	2.26
Sr(1)	+2	2.02
Sr(2)	+2	2.06
Sr(3)	+2	2.02
Sr(4)	+2	2.06

Fig. 4. Comparison between the (a) $[Pt_4O_{10}^{8-}]_\infty$ column in $Sr_4PbPt_4O_{11}$ and (b) the $[Pt_4O_8^{4-}]_\infty$ columns $CaPt_2O_4$.
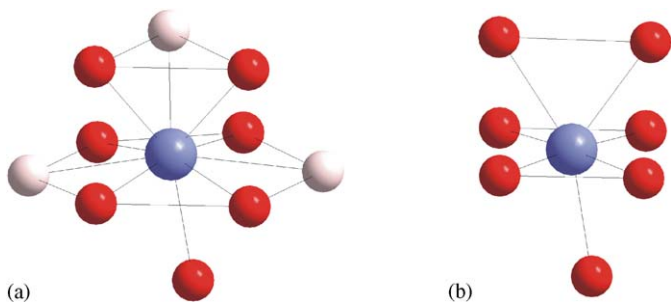
Fig. 5. Strontium environments; (a) ten coordinated Sr(2) and Sr(4), the light oxygen atoms are the axial oxygen of the PtO_5 pyramid and (b) seven coordinated Sr(1) and Sr(3).

from the pyramid apex. There is a close resemblance between the Sr(2) or Sr(4) environments and the 12 coordination observed in hexagonal-type perovskite built from the stacking of $[SrO_3]$ layers, one equilateral triangle distributed oxygen atoms of the 12 coordination are replaced by one oxygen atom in the 10 coordination.

The lead atoms link two columns via the pyramidal axial oxygen atoms O(5) and O(11) and complete their coordination environment with a third oxygen atom O(10) located between the lead atoms along [100] (Fig. 3c). Then, the lead atoms are three coordinated with Pb–O distances between 2.200(4) and 2.229(4) Å and O–Pb–O angles around $95°$ (Table 4). Such an asymmetric Pb^{2+} coordination environment is observed, for example, in alkaline metal lead oxides A_4PbO_3 (A = K, Rb, Cs) [43–45] with Pb^{2+}–O distances ranging from 2.10 to 2.20 Å and O–Pb–O angle close to $95°$. Indeed, the lone pair E of

Pb^{2+} complete the environment to form a more usual PbO_3E tetrahedron.

3.4. Bond valence calculation

In opposite to organic chemistry, there are various models for chemical bonds in inorganic chemistry. The concept of bond valence [46] provides a useful description largely used in solid state chemistry; in this model, all atoms are considered as cations or anions. The bond valence sums for all cations in $Sr_4PbPt_4O_{11}$ (Table 5) were calculated using the bond valence parameters R_0 from Brese and O'Keeffe data [47] with the formula $s = \exp[(R_0 - R)/b]$ and $b = 0.37$. These results unambiguously confirm that Sr and Pb are divalent. For platinum atoms the valence bond sums calculations using $R_0 = 1.768$ for Pt^{II} and $R_0 = 1.879$ for Pt^{IV} indicate that the four-coordinated Pt(1) and Pt(4) atoms are clearly divalent, which is an usual oxidation state for this coordination. Actually, it can vary from +2, for example in MPt_3O_4 (M = Mn, Co, Zn, Mg, Ni) [48], to +3 in columnar-staked PtO_4 as in $PbPt_2O_4$ [3] and can even take a non-integer mean value like in $Na_xPt_3O_4$ [38–40]. For the five-coordinated Pt atoms, Pt(2) and Pt(3), the valence bond sums are 2.57 if these atoms are supposed to be divalent and 3.46 if they are supposed to be tetravalent. Calculating that the mean oxidation state of platinum is +3 in $Sr_4PbPt_4O_{11}$, and the square pyramid to planar square ratio is 1, one can suppose that Pt(2) and Pt(3) are Pt^{IV} in better agreement with the bond valence calculations results.

All the oxygen atoms are penta-coordinated by two Pt and three Sr atoms (O(1) to O(4) and O(6) to O(9)), one Pt, three Sr and one Pb ((O(5) and O(11)) and four Sr and one Pb (O(10)). The valence bond sums are in the range from 1.71 to 2.10 v.u., it is noticeable that the lowest values correspond to O atoms connected to only divalent Pt.

3.5. Vibrational spectroscopy

In order to point up the unusual pyramidal environment of the platinum, we have undertaken a Raman spectroscopy investigation. To identify the fingerprint of this platinum conformation, we have synthesized the three platinum oxide compounds: Sr_4PtO_6, $Bi_{1.6}Pb_{0.4}PtO_4$ and $PbPt_2O_4$. The crystallographic data of Sr_4PtO_6 [10] show regular PtO_6 octahedral entities linked together through strontium cations. As the space group is $R\bar{3}c$ (D_{3d}^6) and the platinum atoms lies in $\bar{3}$ (S_6), only the A_{1g}, E_g and F_{2g} internal modes (Fig. 5) are active in Raman scattering while F_{1u} species are not allowed. $Bi_{1.6}Pb_{0.4}PtO_4$ is described in a $P4/ncc$ (D_{4h}^8) space group [5] where platinum and oxygen atoms form columns of square planes bonded together through lead or bismuth ions. Active modes for square are A_{1g}, B_{2g} and B_{1g}. $PbPt_2O_4$ cell [3] contains PtO_6 octahedra and PtO_4 square units sharing corners or edges. The vibration motion correspondence between octahedral, square plane and square pyramid conformations is reported in Fig. 6. The principal differences between the various environments lie in the axial stretching vibration mode that is missing or forbidden in the square plane and octahedron while it is active in the square pyramid. Fig. 7 exhibits the Raman spectra of the Sr_4PtO_6, $Bi_{1.6}Pb_{0.4}PtO_4$ and $PbPt_2O_4$ references and of our $Sr_4PbPt_4O_{11}$ compound.

In the literature [49–51], we find the stretching motion of Pt–O bond in the 450–700 cm^{-1} frequency range. In this expecting spectral domain, we observe the stretching Pt–O motion at 631 cm^{-1} for $Bi_{1.6}Pb_{0.4}PtO_4$ in which the square plane is the unique platinum environment. We can note the lower frequency values of the stretching motions in the PtO_6 octahedral species in Sr_4PtO_6 structure. The three compounds $Bi_{1.6}Pb_{0.4}PtO_4$, $PbPt_2O_4$ and $Sr_4PbPt_4O_{11}$ contain PtO_4 square plane units. By comparison, we can
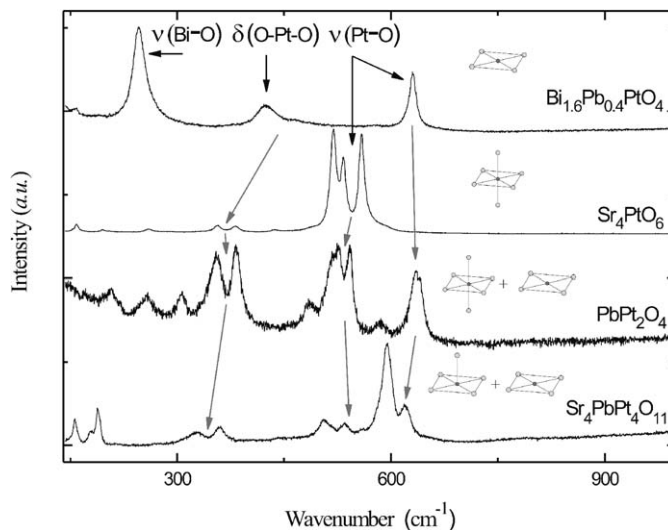
Fig. 7. Raman spectra of $Bi_{1.6}Pb_{0.4}PtO_4$, Sr_4PtO_6, $PbPt_2O_4$ and $Sr_4PbPt_4O_{11}$. The specific platinum coordination environments are recalled for each compound.

Fig. 6. Correspondence between stretching and bending vibration modes in octahedral, square plane and square pyramid units. Only active modes of the octahedron have been represented except F_{1u} species, not allowed in Raman spectroscopy but indicated for the comparison with the axial stretching motion of the square pyramid.
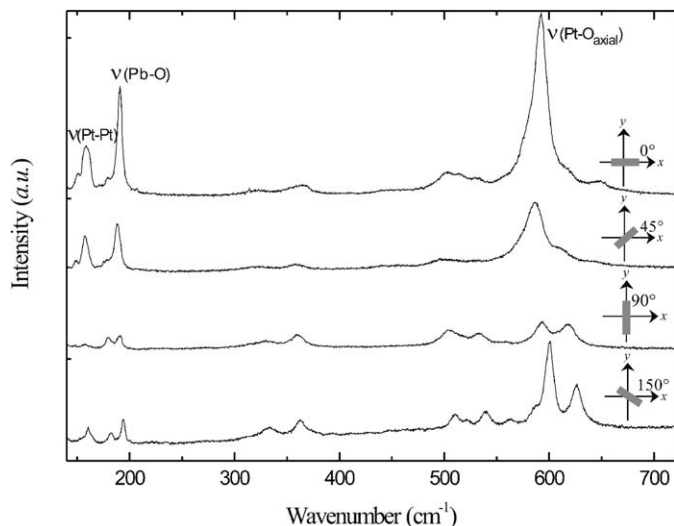
assign Pt–O square plane stretching vibration modes to the bands at 631 cm^{-1} in $Bi_{1.6}Pb_{0.4}PtO_4$, 635, 640 in $PbPt_2O_4$, and 620 cm^{-1} in $Sr_4PbPt_4O_{11}$. As the octahedron can be seen as a square bipyramid, common vibrational motions can be expected in the simple square pyramid and the bipyramid. Thus, the lines at 519, 533 and 559 cm^{-1} in Sr_4PtO_6 are observed at 520, 526 and 542 cm^{-1} in $PbPt_2O_4$ and at 506, 536 and 560 cm^{-1} in $Sr_4PbPt_4O_{11}$. The slight frequency shifts can be explained by the various polyhedral interactions. The specificity of $Sr_4PbPt_4O_{11}$ spectrum lies in its more intense band at 594 cm^{-1}. This line, located between the octahedral and square plane stretching frequencies, characterizes the square pyramid, and is attributed to the axial Pt–O stretching vibration mode. This vibrational motion, not allowed in the octahedron and missing in the square plane (Fig. 6), becomes active in the square pyramidal conformation. The O–Pt–O angular deformation corresponds to the same vibrational motion for all the conformations. The observed frequency shifts are due to different polyhedral interactions. They are located at 424 and 468 cm^{-1} in $Bi_{1.6}Pb_{0.4}PtO_4$, 356 and 382 cm^{-1} in Sr_4PtO_6, 356 and 383 cm^{-1} in $PbPt_2O_4$ and 329 and 360 cm^{-1} in $Sr_4PbPt_4O_{11}$. For $Bi_{1.6}Pb_{0.4}PtO_4$, we have assigned the strong intense band at 246 cm^{-1} to Bi–O stretching motion [52]. The Raman spectroscopy has thus evidenced the unusual square pyramidal environment of the platinum atoms by identifying the 594 cm^{-1} frequency band as the fingerprint of this coordination. Furthermore, in complexes containing a discrete Pt–Pt bond a Raman active band characteristic of the Pt–Pt stretching vibration is observed near 150 cm^{-1} [53–55]. Notably, the metal–metal stretching frequency is observed at 144 cm^{-1} in $[Pt_2Cl_2(acac)_4]$ [54] and 145 cm^{-1} in $[Pt_2(CN)_{10}]^{4-}$ [55] for 2.70 Å and 2.73 Å Pt–Pt distances, respectively. The metal–metal distances are shorter (2.6712(3) and

Fig. 8. Polarized Raman spectra of $Sr_4PbPt_4O_{11}$ single crystal obtained for different crystal orientation specified for each spectrum.

2.6613(3) Å) in $Sr_4PbPt_4O_{11}$ thus, the observed band at $156 \, cm^{-1}$ in $Sr_4PbPt_4O_{11}$ can reasonably be attributed to the Pt–Pt vibration. Furthermore, the Pt_2 bond forms the last direction of an octahedron within PtO_5 square pyramid, therefore the same polarization can be expected for the axial Pt–O and Pt–Pt stretching motion. Fig. 8 shows Raman spectra of $Sr_4PbPt_4O_{11}$ single crystals recorded with different needle orientations. Same order of depolarization ratio is obtained for the band at $594 \, cm^{-1}$ (axial Pt–O stretching vibration) and the bands at 156, 179 and $188 \, cm^{-1}$, the slight frequency shifts observed for the different orientation are due to the different components making the bands. The intensity of the bands corresponding to the stretching motions perpendicular to the needle axis, [100], does not change in the horizontal orientation while it decreases in the vertical one. The polarization effects confirm the 156 and $594 \, cm^{-1}$ band attribution to v(Pt–Pt) and v(Pt–O_{axial}). The lines at 179, $188 \, cm^{-1}$ are assigned to the Pb–O stretching vibration, two of the three Pb–O bonds are perpendicular to a-axis and the wavenumber value is in good agreement with literature [56].

3.6. Thermal stability

DTA experiment showed that $Sr_4PbPt_4O_{11}$ is stable under air up to 950 °C, at this temperature it decomposes to a mixture of Sr_4PtO_6, Pt and PbO.

4. Conclusion

The new $Sr_4PbPt_4O_{11}$ compound presents an original structure within platinum atoms in the unusual square pyramidal coordination and contains dinuclear metal–metal bonded Pt_2^{6+} ions evidenced for the first time in a platinum oxide. Synthesis of other oxides containing isolated dinuclear ions for platinum but also for other metals such as rhodium are expected in a next future.

References

[1] K.B. Schwartz, C.T. Prewitt, J. Phys. Chem. Solids 45 (1) (1984) 1.
[2] N. Bettahar, P. Conflant, F. Abraham, D. Thomas, J. Solid State Chem. 67 (1987) 85.
[3] N. Tancret, S. Obbade, N. Bettahar, F. Abraham, J. Solid State Chem. 124 (1996) 309.
[4] S. Obbade, N. Tancret, F. Abraham, E. Suard, J. Solid State Chem. 166 (2002) 58.
[5] J.C. Boivin, P. Conflant, D. Thomas, Mater. Res. Bull. 11 (1976) 1503.
[6] N. Bettahar, P. Conflant, J.C. Boivin, F. Abraham, D. Thomas, J. Chem. Phys. Solids 46 (1985) 297.
[7] N. Bettahar, P. Conflant, F. Abraham, J. Alloys Compounds 188 (1992) 211.
[8] P. Conflant, J.C. Boivin, D. Thomas, Rev. Chem. Miner. 14 (1977) 249.
[9] J.C. Boivin, J. Tréhoux, D. Thomas, Bull. Soc. Fr. Miner. Crystallogr. 99 (1976) 193.
[10] J.J. Randall, R. Ward, J. Am. Chem. Soc. 81 (1959) 2629.
[11] J.J. Randall, R. Ward, Acta Crystallogr. 12 (1959) 519.
[12] I. Ben-Dor, J.T. Suss, S. Cohen, J. Cryst. Growth 64 (1983) 395.
[13] P. Nunez, S. Trail, H.-C. zur Loye, J. Solid State Chem. 130 (1997) 35.
[14] M.D. Smith, H.-C. zur Loye, Acta Crystallogr. E 59 (2003) i75.
[15] T.N. Nguyen, D.M. Giaquinta, H.-C. zur Loye, Chem. Mater. 6 (1994) 1642.
[16] J.B. Claridge, R.C. Layland, W.H. Henley, H.-C. zur Loye, Chem. Mater. 11 (1999) 1376.
[17] A.P. Wilkinson, A.K. Cheetham, W.K. Kunnmann, A. Kvick, Eur. J Solid State Inorg. Chem. 28 (1991) 453.
[18] J.L. Hodeau, H.Y. Tu, P. Bordet, T. Fournier, P. Strobel, M. Marezio, G.V. Chandrashekhar, Acta Crystallogr. B 48 (1992) 1.
[19] C. Lampe-Önnerud, H.-C. zur Loye, Inorg. Chem. 35 (1996) 2155.
[20] SAINT version 7.06a, Bruker AXS Inc., Madison, Wisconsin, USA, 2004.
[21] SADABS 2004/1, Bruker AXS Inc., Madison, Wisconsin, USA, 2004.
[22] A. Altomare, M.C. Burla, M. Camalli, G. Cascarano, C. Giacovazzo, A. Guagliardi, A.G.G. Moliterni, G. Polidori, R. Spagna, SIR97, A Package for Crystal Structure Solution by Direct Methods and Refinement, Bari, Rome, Italy, 1997.
[23] V. Petricek, M. Dusek, L. Palatinus, Jana2000, Structure Determination Software Programs, Institute of Physics, Praha, Czech Republic, 2005.
[24] J.P. Becker, P. Coppens, Acta Crystallogr. A 30 (1974) 148.
[25] I. Garcia-Seijo, A. Habtemariam, P. del Socorro Murdoch, R.O. Gould, M.E. Garcia-Fernandez, Inorg. Chim. Acta 335 (2002) 52.
[26] S. Aizawa, T. Kobayashi, T. Kawamoto, Inorg. Chim. Acta 358 (2005) 2319.
[27] I. Ara, J. Fornies, M.A. Garcia-Monforte, B. Menjon, R.M. Sanz-Carrillo, M. Tomas, A.C. Tsipis, C.A. Tsipis, Chem. Eur. J. 9 (2003) 4094.

[28] J.P. Besse, G. Baud, R. Chevalier, M. Gasperin, Acta Crystallogr. B 34 (1978) 3532.

[29] K. Waltersson, Acta Crystallogr. B 32 (1976) 1485.

[30] M. Pley, M.S. Wickleder, Z. Anorg. Allg. Chem. 630 (2004) 1036.

[31] F.A. Cotton, L.R. Falvello, S. Han, Inorg. Chem. 21 (1982) 2889.

[32] D.P. Bancroft, F.A. Cotton, L.R. Falvello, S. Han, W. Schwotzer, Inorg. Chim. Acta 87 (1984) 147.

[33] R. El-Mehdawi, F.R. Frontczek, D.M. Roundhill, Inorg. Chem. 25 (1986) 1155.

[34] H.L. Conder, F.A. Cotton, L.R. Falvello, S. Han, R.A. Walton, Inorg. Chem. 22 (1983) 1887.

[35] D.M. Roundhill, H.B. Gray, C.-M. Che, Acc. Chem. Res. 22 (1989) 55.

[36] L.A.M. Baxter, G.A. Heath, R.G. Raptis, A.C. Willis, J. Am. Chem. Soc. 114 (1992) 6944.

[37] R. Cini, F.P. Fanizzi, F.P. Intini, G. Natile, J. Am. Chem. Soc. 113 (1991) 7805.

[38] K.B. Schwartz, J.B. Parise, C.T. Prewitt, R.D. Shannon, Acta Crystallogr. B 38 (1982) 2109.

[39] R.D. Shannon, T.E. Gier, P.F. Garcia, P.E. Bierstedt, R.B. Flippen, A.J. Vega, Inorg. Chem. 21 (1982) 3372.

[40] K.B. Schwartz, C.T. Prewitt, R.D. Shannon, L.M. Corliss, J.M. Hastings, B.L. Chamberland, Acta Crystallogr. B 38 (1982) 363.

[41] W.J. Moore, L. Pauling, J. Am. Chem. Soc. 63 (1941) 1392.

[42] D. Cahen, J.A. Ibers, M.H. Mueller, Inorg. Chem. 13 (1974) 110.

[43] K.P. Martens, R.Z. Hoppe, Z. Anorg. Allgem. Chem. 440 (1978) 81.

[44] R. Brandes, R. Hoppe, Z. Anorg. Allgem. Chem. 620 (1994) 1549.

[45] H. Stoll, B. Brazel, R. Hoppe, Z. Anorg. Allgem. Chem. 564 (1988) 45.

[46] I.D. Brown, Chem. Soc. Rev. 7 (1978) 359.

[47] E. Brese, M. O'Keeffe, Acta Crystallogr. B 47 (1991) 192.

[48] K.B. Schwartz, J.B. Parise, C.T. Prewitt, R.D. Shannon, Acta Crystallogr. B 39 (1983) 217.

[49] W.H. Weber, G.W. Graham, A.E. Chen, K.C. Hass, B.L. Chamberland, Solid State Commun. 106 (1998) 95.

[50] W.H. Weber, G.W. Graham, J.R. McBride, Phys. Rev. B 42 (1990) 10969.

[51] G.W. Graham, W.H. Weber, J.R. McBride, C.R. Peters, J. Raman Spectrosc. 22 (1991) 1.

[52] F.D. Hardcastle, I.E. Wachs, J. Solid State Chem. 97 (1992) 319.

[53] P.D. Harvey, K.D. Truong, K.T. Aye, M. Drouin, A.D. Bandrauk, Inorg. Chem. 33 (1994) 2347.

[54] P.D. Penzler, G.A. Heath, R.G. Raptis, Chem. Commun. 15 (1996) 2271.

[55] F. Jalilehvand, M. Maliarik, J. Mink, M. Sandström, A. Ilyukhin, J. Glaser, J. Phys. Chem. A 106 (2002) 3501.

[56] V.N. Sigaev, I. Gregora, P. Pernice, B. Champagnon, E.N. Smelyanskaya, A. Aronne, P.D. Sarkisov, J. Non-Cryst. Solids 279 (2001) 136.